

NASA CR- 144766



(NASA-CR-144766) EXTREME SOLAR ULTRAVIOLET
MONITOR (ESUM) FOR ATMOSPHERE EXPLORER (Ball
Bros. Research Corp.) 59 p HC \$4.50

N76-29361

CSSL 14B

Unclas
48575

G3/19



Aerospace Division

Ball Brothers Research Corporation



Final Report

Extreme Solar Ultraviolet Monitor
(ESUM)

for

Atmosphere Explorer

F76-10

1 April 1976

Prepared For:

National Aeronautics and Space Administration
Goddard Space Flight Center
Greenbelt, Maryland

Contract No.: NAS5-11441



Aerospace Division
Ball Brothers Research Corporation

SUBSIDIARY OF BALL CORPORATION
BOULDER, COLORADO 80302



Final Report

Extreme Solar Ultraviolet Monitor
(ESUM)

for

Atmosphere Explorer

F76-10

1 April 1976

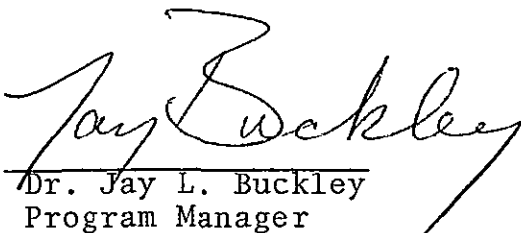
Prepared for:

National Aeronautics and Space Administration

Goddard Space Flight Center

Greenbelt, Maryland

Contract No.: NAS5-11441

A handwritten signature in cursive script, reading "Jay L. Buckley".
Dr. Jay L. Buckley
Program Manager

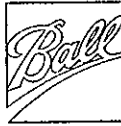


TABLE OF CONTENTS

<u>SECTION</u>	<u>TITLE</u>	<u>PAGE</u>
1.0	SCOPE	1-1
2.0	REFERENCE DOCUMENTS	2-1
3.0	INSTRUMENT SUMMARY	3-1
3.1	Overview	3-1
3.2	Objectives	3-1
3.3	ESUM-C	3-2
3.4	ESUM-E	3-3
4.0	ELECTRONIC CALIBRATION	4-1
4.1	ESUM-C SEM Electronics	4-1
4.1.1	Preamplifiers	4-1
4.1.2	Discriminator Thresholds	4-1
4.1.3	Pulse Pair Resolution and Pile-Up	4-1
4.2	ESUM-C Diode Electronics	4-2
4.2.1	General	4-2
4.2.2	Electrometers	4-2
4.2.3	Gain Change Amplifiers	4-3
4.2.4	Internal Calibration	4-4
4.3	ESUM-E Diode Electronics	4-5
4.3.1	General	4-5
4.3.2	Electrometers	4-5
4.3.3	Gain Change Amplifiers	4-6
4.3.4	Internal Calibration	4-6
4.3.5	Noise and Offset	4-7



TABLE OF CONTENTS
(Continued)

<u>SECTION</u>	<u>TITLE</u>	<u>PAGE</u>
5.0	PHOTOMETRIC CALIBRATION	5-1
5.1	General	5-1
5.2	ESUM-C Calibration Data	5-2
5.2.1	ESUM-C SEMs	5-2
5.2.2	ESUM-C EUV Diodes	5-2
5.3	ESUM-E	5-2
5.3.1	EUV Diodes for ESUM-E	5-2
5.3.2	Visible Light Diode for ESUM-E	5-16
6.0	INSTRUMENT PHOTOMETRIC TESTS	
6.1	General	6-1
6.2	Testing of ESUM-C	6-2
6.2.1	Test Configuration	6-2
6.2.2	ESUM-C Testing of 27 September 1973	6-2
6.2.3	ESUM-C Test Results of 1 November 1973	6-7
6.3	ESUM-E Photometric Testing	6-12
6.3.1	General	6-12
6.3.2	ESUM-E Photometric Tests January/February 1975	6-12



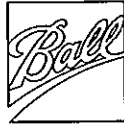
ILLUSTRATIONS

	TITLE	PAGE
Figure 3.3.1	Overall View of ESUM-C Configuration	3-4
Figure 3.3.2	Detector Head Optical/Mechanical Assembly	3-5
Table 3.4.1	Spectral Response Characteristics of ESUM-E	3-6
Figure 3.4.1	Front View of ESUM-E with Redesigned Mask Installed	3-7
Figure 3.4.2	Optical Layout of Mask, Filter, and Diode Geometry for ESUM-E	3-8
Table 4.2.1	Measured Transresistance Values	4-3
Figure 5.2.1	Final Data for Flight SEM, Position 1	5-3
Figure 5.2.2	Final Data for Flight SEM, Position 2	5-4
Figure 5.2.3	Final Data for Flight SEM, Position 3	5-5
Figure 5.2.4	Final Data for Flight SEM, Position 4	5-6
Figure 5.2.5	Calibration Curve for the ESUM-C EUV Diodes, Position 1	5-7
Figure 5.2.6	Calibration Curve for the ESUM-C EUV Diodes, Position 2	5-8
Figure 5.2.7	Calibration Curve for the ESUM-C EUV Diodes, Position 3	5-9
Figure 5.3.1	NBS Calibration Reports	5-10
Table 6.2.1	ESUM-C Photometric Tests of 27 September 1973	6-3
Table 6.2.2	Results of Photometric Tests	6-5
Table 6.2.3	Results of High Voltage Level Tests	6-6
Table 6.2.4	ESUM-C Photometric Tests of 1 November 1973	6-8



ILLUSTRATIONS
(Continued)

	TITLE	PAGE
Table 6.2.5	Data Collected During Runs 1-21 on 1 November 1973	6-9
Table 6.2.6	Results of 10 Filter Wheel Revolutions Sampled in Run 22	6-11
Table 6.3.1	ESUM-E T-V/Cal Tests 1975	6-13
Table 6.3.2	ESUM Calibration Summary	6-16
Table 6.3.3	ESUM Calibration Summary	6-19



1.0 SCOPE

This document describes the performance and calibration of the Extreme Solar Ultraviolet Monitor (ESUM) for Atmosphere Explorer-C (AE-C) and Atmosphere Explorer-E (AE-E).

This work was performed by Ball Brothers Research Corporation (BBRC) for the Goddard Space Flight Center (GSFC) under contract NAS5-11441.



2.0

REFERENCE DOCUMENTS

S-652-P-1 "GSFC Specification - Extreme Solar Ultraviolet Monitor for the Atmosphere Explorer AE-C, -D and -E." August 1971 plus revisions.

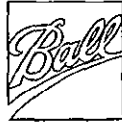
"Preliminary Design Review Report for ESUM", Ball Brothers Research Corporation, 12 October 1971.

"Final Design Report for ESUM", Ball Brothers Research Corporation, 21 June 1972.

"An Extreme UV Photometer for Solar Observations from Atmosphere Explorer", D. F. Heath and J. F. Osantowski, Radio Science, 8, P. 361, April 1973.

Ball Brothers Research Corporation drawing 39479

"Extreme Solar UV Monitor" and its subtier drawings.



3.0 INSTRUMENT SUMMARY

3.1 OVERVIEW

BBRC development of the ESUM instrumentation began June 15, 1971. A prototype unit was assembled and tested over the following twenty months. Design improvements were made, and Flight Unit #1 (FU1) fabrication started in the spring of 1973. FU1 was launched on AE-C in December of 1973.

Following a re-assessment of AE Project priorities, it was decided to refurbish and simplify the Prototype ESUM for flight on AE-E. This activity began in the summer of 1974 and continued through AE-E launch 19 November 1975.

The major change between FU1 and the rebuilt Prototype (FU2) is in the detector complement. Where FU1 had four Spiral Electron Multipliers (SEMs) behind the filter wheel and three fixed Extreme Ultra-Violet photodiodes (EUV Diodes), the rebuilt Prototype had no SEMs and only two EUV Diodes, repositioned to replace the SEMs behind the filter wheel.

For clarity, we designate the two versions of the instrument as ESUM-C and ESUM-E.

This report discusses the design, operation, and calibration of both ESUM-C and ESUM-E. Heath and Osantowski (Radio Science, 8, P. 361, April 1973) provide a comprehensive description of the objectives, system design, and function of the ESUM-C, most of which applies to the ESUM-E as well.

3.2 OBJECTIVES

The principal objective of ESUM is to measure accurately the solar intensity from 40 to 1250 Å during the Atmosphere Explorer



mission. Solar EUV radiation interacts with the Earth's upper atmosphere by ionizing neutral atoms and molecules at altitudes of about 100 to 300 km. The energetic primary ions and electrons then diffuse to form the ionospheric F-layers and supply thermal energy to the entire upper atmosphere. The magnitude of the solar flux is therefore of fundamental importance in the analysis of the structure and dynamics of the upper atmosphere.

The solar EUV spectrum is composed largely of emission lines from multiply-ionized atoms and is greatly affected by changes in solar activity. These changes are directly applied to primary ionization rates, and have time-dependent effects on atmospheric temperature, density and composition profiles. ESUM will monitor the changing solar output (both short term and long term) to increase our understanding of the sun, and to allow meaningful comparative analyses of the atmospheric parameters measured by other instruments in the Atmosphere Explorer payload.

3.3 ESUM-C

ESUM-C measures the sun's output through six spectral regions spanning the wavelength range 40 to 1250 Å. Spectral selection is provided by thin metallic films supported on metal mesh and mounted in an eight position step-rotating filter wheel. Four Spiral Electron Multiplier (SEM) detectors are located behind the filters and as the wheel is stepped, each detector will observe the sun through all six filter positions in sequence. The seventh position is an opaque segment of the wheel for background counts and the final position is a radioactive calibration source (Fe^{55}) for gain and efficiency calibration. A fifth detector position is taken by a visible-sensitive photocell which monitors the integrity of the thin metal filters.

Three fixed EUV photodiodes with aluminum oxide photocathodes complement the SEM/filter wheel system. These three detectors have aluminum, indium, and open filters respectively and provide stable, reliable monitoring of three solar spectral regions.



Figure 3.3.1 provides an overall view of the ESUM-C configuration. Figure 3.3.2 shows a more detailed picture of the Detector Head optical/mechanical assembly.

Table 3.3.1 summarized the spectral response characteristics of the ESUM-C filters and detectors.

Table 3.3.1
Spectral Response Characteristics
of ESUM-C

<u>Filter</u>	<u>Detector</u>	<u>50% Wavelength (Solar)</u>
Aluminum + Carbon	SEM	240 to 303 A
Aluminum	SEM, Diode	270 to 550 A
Titanium	SEM	365 to 535 A
Tin	SEM	570 to 584 A
Indium	SEM, Diode	800 to 935 A
Open	Diode	1216 A

3.4 ESUM-E

ESUM-E measures only four spectral regions, as listed in Table 3.4.1. However, each spectral range is covered twice on the eight position filter wheel.

Figure 3.4.1 shows the front view of ESUM-E with the redesigned mask installed. Grids are seen over the positions of the two EUV Diodes. A clear window covers the Visible Light Diode, at 90° to the two EUV Diodes. A similar clear window covers a sun sensor at the periphery of the mask.

Figure 3.4.2 is an optical layout of the mask, filter, and diode geometry for ESUM-E.

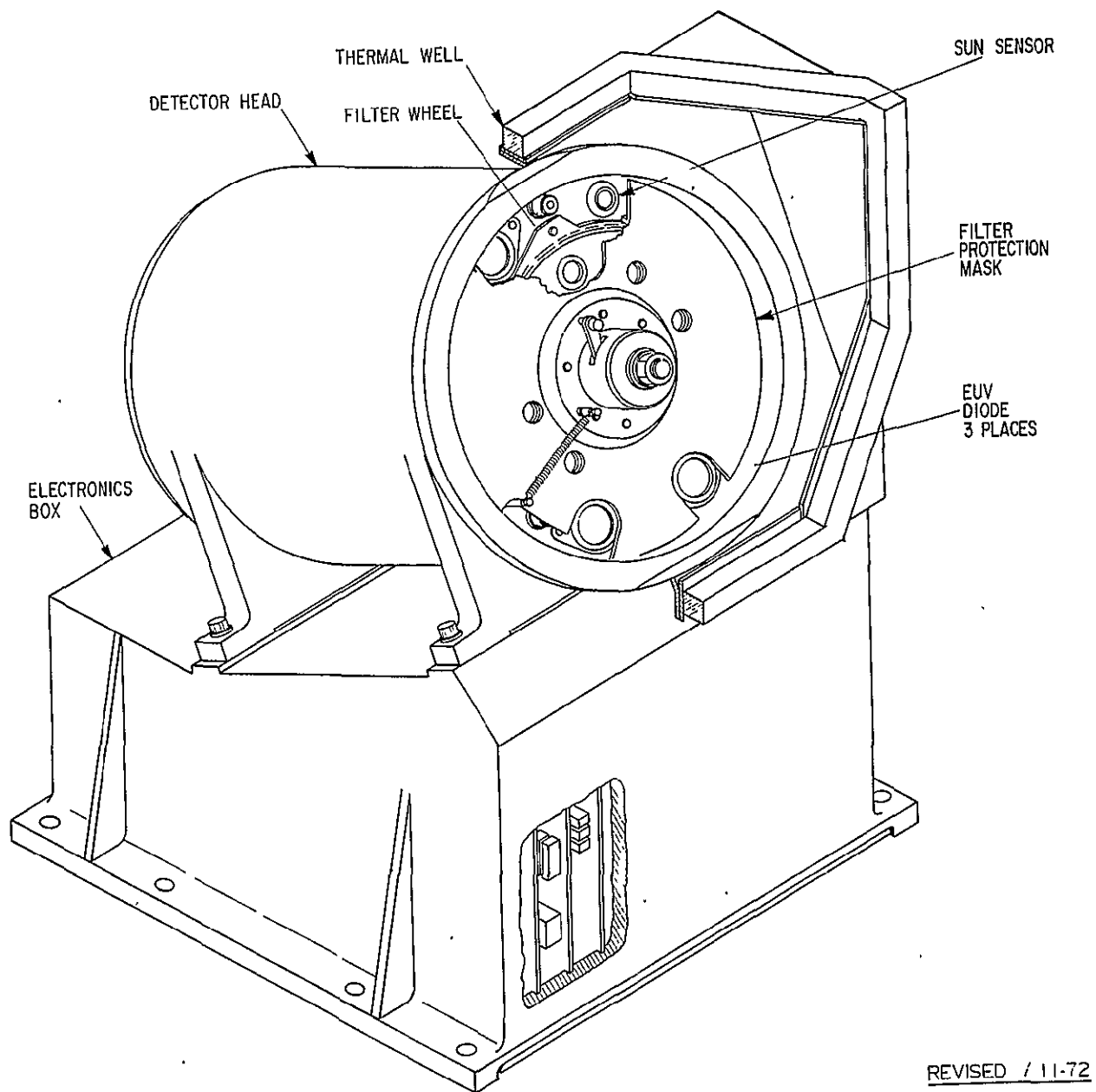


Figure 3.3.1 Overall View of ESUM-C Configuration

ORIGINAL PAGE IS
OF POOR QUALITY



Figure 3.3.2 Detector Head Optical/Mechanical Assembly



TABLE 3.4.1
Spectral Response Characteristics
of ESUM-E

<u>Filter</u>	<u>Detector</u>	<u>50% Wavelength (Solar)</u>
Aluminum	Diode	270 to 550 Å
Tin	Diode	570 to 584 Å
Indium	Diode	800 to 935 Å
No Filter	Diode	1216 Å

ORIGINAL PAGE IS
OF POOR QUALITY

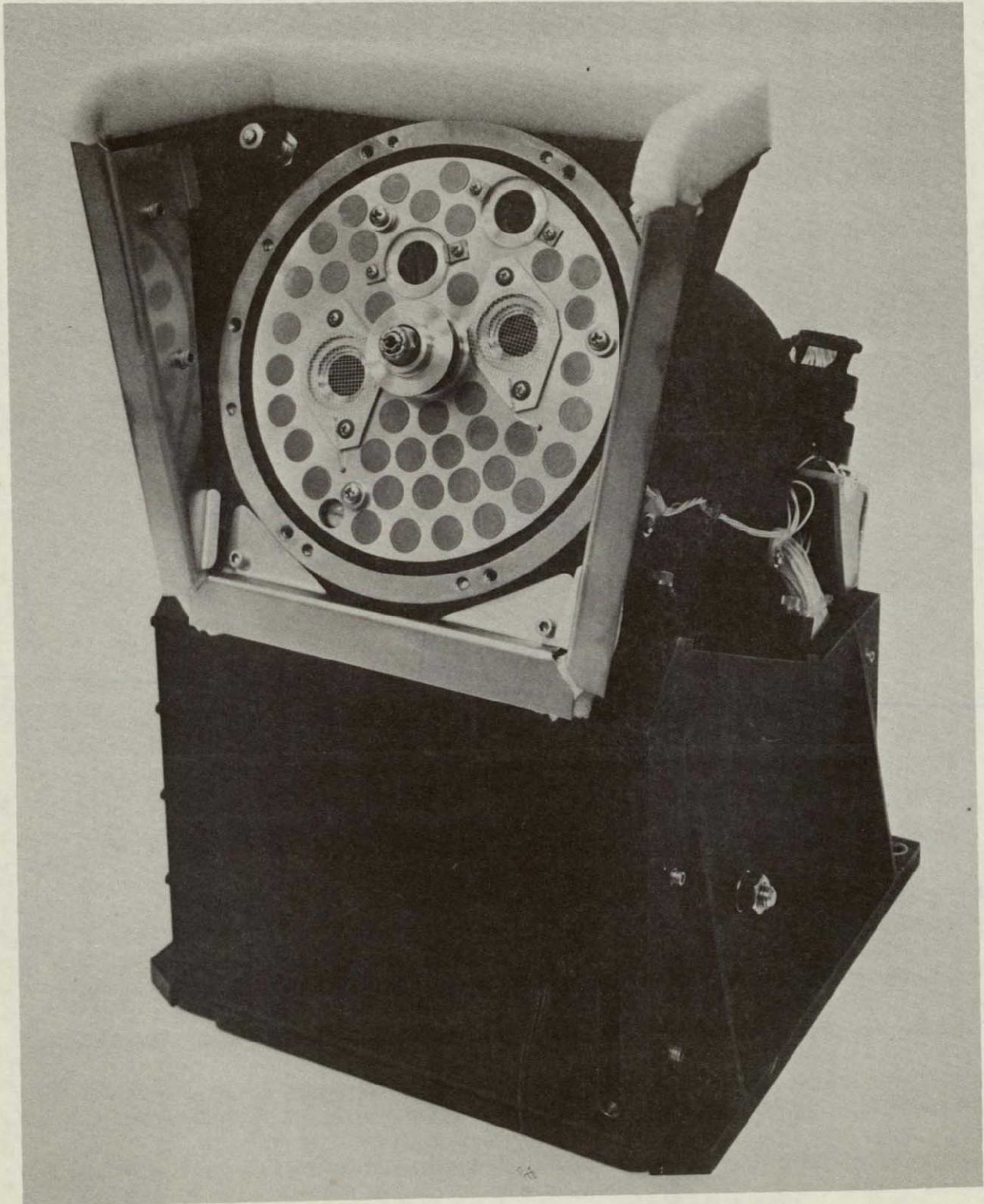


Figure 3.4.1 Front View of ESUM-E With Redesigned Mask Installed

ORIGINAL PAGE IS
OF POOR QUALITY

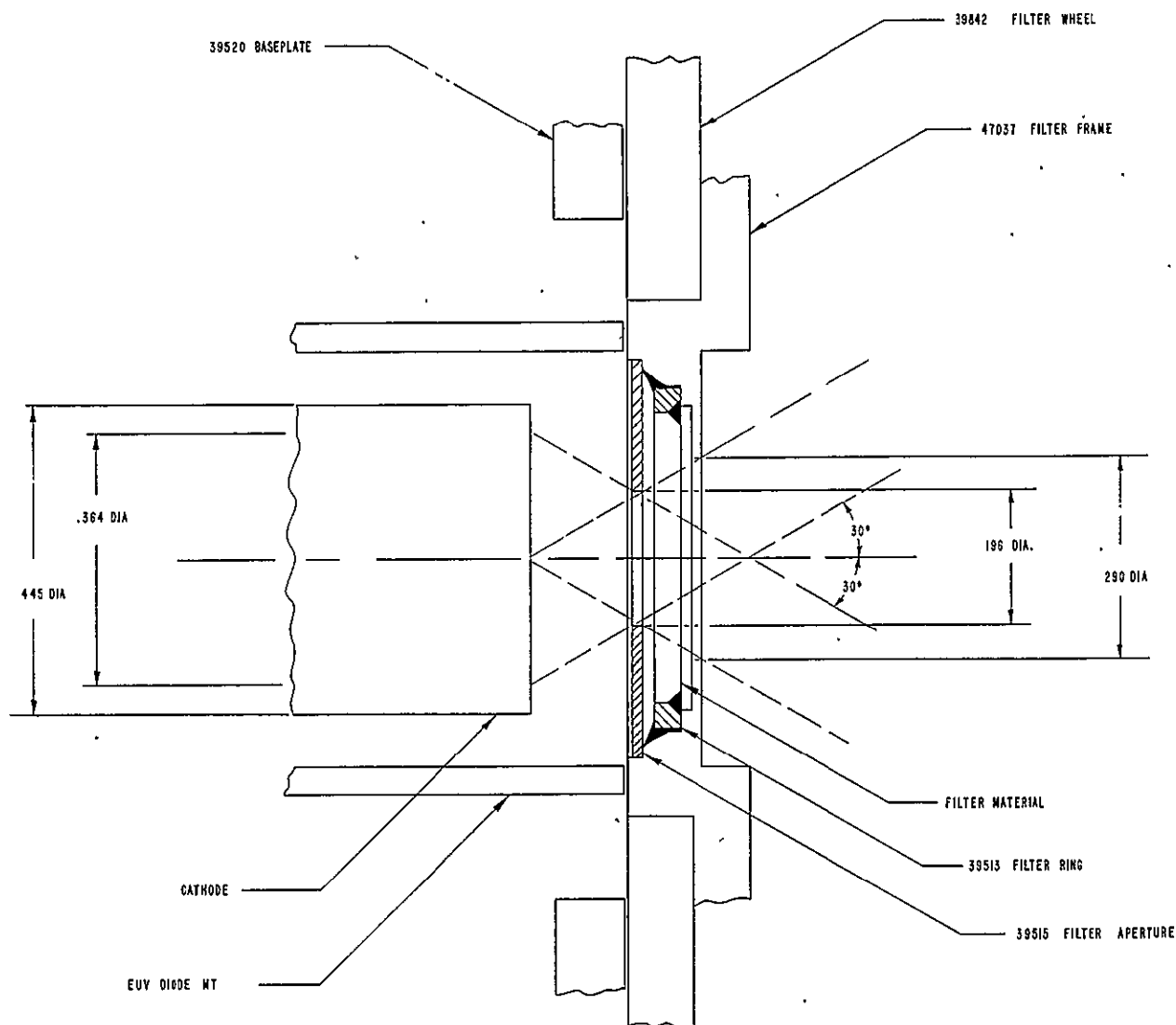


Figure 3.4.2 Optical Layout of Mask, Filter, and Diode Geometry for ESUM-E



4.0 ELECTRONIC CALIBRATION

4.1 ESUM-C SEM ELECTRONICS

4.1.1 Preamplifiers

The SEM pre-amps convert SEM charge pulses to low impedance voltage pulses. The preamp output pulse amplitude is linear with charge up to saturation (8.0 volts out for 1×10^8 electrons in). Normal SEM pulses are 1 to 5×10^8 electrons each, so the preamps are saturated for typical operation.

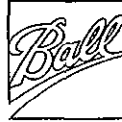
4.1.2 Discriminator Thresholds

The SEM discriminators are set up to count all pre-amp pulses above 30 mv. This corresponds to 3×10^5 electrons. A higher discriminator threshold, corresponding to 1.2 volts (10^7 electrons) is available during commanded calibration sequences, to check SEM operation and provide a safety factor in the event of unexpectedly high spacecraft noise.

4.1.3 Pulse Pair Resolution and Pile-Up

The various electronic time constants combine to give ESUM the capability of resolving (counting) two pulses of 10^8 electrons separated by about one microsecond. Larger amplitude pulses will tend to broaden slightly. However, for the predicted 10^4 per second count rates, we expect no appreciable non-linearities.

The ESUM discriminators are saturating analog amplifiers, rather than true "one shot's". Thus an extremely high count rate (say 5×10^6 per second random), will saturate the discriminators except for the statistical gaps in the pulses. In this case, the unit is counting "holes" rather than counts. Such behavior is a problem when testing the instrument if a UV source of excessive intensity is used.



4.2 ESUM-C DIODE ELECTRONICS

4.2.1 General

Diode currents are measured by a system of high sensitivity electrometers and gain changing analog amplifiers. The electrometers develop a voltage output equal to the voltage generated by the diode current passing through a high impedance input resistor (10^9 ohms for EUV diode #1, 10^{10} ohms for EUV diodes 2 and 3 and 10^7 ohms for visible light diode).

The gain-change amplifiers have 7 ranges. The most sensitive range has a voltage gain of 63.6 for EUV diode #1, 199 for the other three diodes. Gain is reduced by a factor of two for each range change.

The range state (R) is presented directly to the spacecraft telemetry system. The amplifier output voltage goes to an 8-bit A/D converter (20 mv/step) for telemetry. Thus diode currents are expressed as a pair of numbers R(1-7) and S(0-255).

A single response time for the diode electronics cannot be defined because gain changing and readouts are controlled by 0.25 second timing pulses. The output from a full-scale current step will stabilize to within one bit within 0.75 seconds.

4.2.2 Electrometers

The voltage out of the electrometers (V) is proportional to the input current (I) and the transresistance (R):

$$V_{\text{out}} = IR + \text{Offset}$$

Offset levels are discussed in Section 4.3.5. Table 4.2.1 gives the measured transresistance values (R) at -20°C , 22°C , and 50°C for the electrometers.



TABLE 4.2.1

Diode	Temperature		
	-20°C	22°C	50°C
1	1.025	1.000	.987 x 10 ⁹ ohm
2	1.020	.990	.978 x 10 ¹⁰ ohm
3	1.025	.995	.985 x 10 ¹⁰ ohm
4	1.000	1.000	1.000 x 10 ⁷ ohm

4.2.3 Gain Change Amplifiers

The electrometer voltages are amplified by the gain changing amplifiers prior to telemetry.

A particular diode current is given by

$$I(\text{amp}) = \frac{.020}{R_i G} * (S * 2^{R-1} - S_o)$$

Where R_i is the electrometer input resistance for the particular electrometer and temperature

G is the electrometer gain on Range 1

S is the digital signal level

R is the digital range level

S_o is the offset signal (no illumination), always on Range 1.

The gains are not exactly a factor of two between range steps.

The following gains were measured for the 4 gain change amplifiers.

Range	Gain for Diode #			
	1	2	3	4 (VLD)
1	63.7	199.2	199.4	199.8
2	31.9	99.6	99.6	100.0
3	15.9	49.8	49.7	49.9
4	7.95	24.8	24.8	24.9
5	3.97	12.38	12.38	12.41
6	1.985	6.18	6.18	6.21
7	1.003	3.13	3.13	3.14



On the Range 1, one A/D step (0.020 volts) corresponds to:

EUV Diode #1:	.020/10 ⁹ /63.6	= 3.144 x 10 ⁻¹³ amps
EUV Diode #2:	.020/10 ¹⁰ /199	= 1.005 x 10 ⁻¹⁴ amps
EUV Diode #3:	.020/10 ¹⁰ /199	= 1.005 x 10 ⁻¹⁴ amps
Vis Light Diode #4:	.020/10 ⁷ /199	= 1.005 x 10 ⁻¹¹ amps

Maximum signal from each electrometer (255 on Range 7) is

EUV Diode #1:	16320 x 3.144 x 10 ⁻¹³	= 5.13 x 10 ⁻⁹ amps
EUV Diode #2:	16320 x 1.005 x 10 ⁻¹⁴	= 1.64 x 10 ⁻¹⁰ amps
EUV Diode #3:	16320 x 1.005 x 10 ⁻¹⁴	= 1.64 x 10 ⁻¹⁰ amps
Vis Light Diode #4:	16320 x 1.005 x 10 ⁻¹⁴	= 1.64 x 10 ⁻⁷ amps

4.2.4 Internal Calibration

The instrument is equipped with an internal current calibration circuit, designed to verify electrometer stability. The calibration current is generated by applying a voltage ramp (-10V to +10V in 10 secs) to a capacitor at the electrometer input.

The current generated by this circuit is given by

$$i = C \frac{dV}{dt} + \frac{V}{R}$$

where

$$\frac{dV}{dt} = 20 \text{ v/sec}$$

$$C = 10 \text{ pf (diodes 1,2,3); } .01 \text{ } \mu\text{f (diode 4)}$$

$$R = \text{leakage resistance of the capacitor}$$

The selected capacitance and voltage ramp give currents in the EUV Diodes of about 5 x 10⁻¹² amps. However, the value of R (10⁻¹⁴ Ω or so) is at the limit of available capacitors, and is expected to change slightly with age and temperature.

By sampling the calibration current near the center of the interval



(near $V = 0$) we get a valid reading $C \frac{dV}{dt}$, independent of leakage resistance.

Injection of the calibrate current does not inhibit normal operation of the diodes, but merely adds current to any photon current being generated.

4.3 ESUM-E DIODE ELECTRONICS

4.3.1 General

The electrometers and gain change amplifiers are identical in design on both ESUM-E and ESUM-C. On ESUM-E, transresistances for both EUV Diodes were set at 10^{10} ohms nominal, and 10^6 ohms for the visible light diode. In the refurbishment of ESUM-E, we used the gain-change amplifiers for EUV Diodes #2 and #3 from the prototype, and we continue to designate the two ESUM-E EUV Diodes by those numbers.

4.3.2 Electrometers

Electrometer transresistance values for ESUM-E were measured as follows

Diode #	Temperature		
	-20°C	22°C	50°C
2	1.042	.998	.987 x 10^{10} ohm
3	1.048	1.011	.989 x 10^{10} ohm
4 (VLD)	1.000	1.000	1.000 x 10^6 ohm



4.3.3 Gain Change Amplifiers

Gain on each range was measured as follows (no significant change with temperature);

<u>Range</u>	<u>2</u>	<u>3</u>	<u>4 (VLD)</u>
1	199.5	199.2	199.4
2	99.5	99.8	99.7
3	49.7	49.7	49.7
4	24.9	24.8	24.9
5	12.5	12.4	12.6
6	6.22	6.20	6.26
7	3.16	3.15	3.17

On Range 1, one A/D step [0.020 volts] corresponds to

$$\text{Diode \#2: } .020/10^{10}/199.5 = 1.003 \times 10^{-14} \text{ amps}$$

$$\text{Diode \#3: } .020/10^{10}/199.2 = 1.004 \times 10^{-14} \text{ amps}$$

$$\text{Diode \#4: } .020/10^6/199.4 = 1.000 \times 10^{-10} \text{ amps}$$

Full scale (Range 7, 255 counts on A/D) is then

$$\text{Diode \#2: } 255 \times .020/10^{10}/3.16 = 1.63 \times 10^{-10} \text{ amps}$$

$$\text{Diode \#3: } 255 \times .020/10^{10}/3.15 = 1.62 \times 10^{-10} \text{ amps}$$

$$\text{Diode \#4: } 255 \times .020/10^6/3.17 = 1.61 \times 10^{-6} \text{ amps}$$

4.3.4 Internal Calibration

The calibration input capacitors for ESUM-E are nominally 10 pf for diodes 2 and 3, and .01 μ f for the visible light diode.

We measured calibration signal levels of

$$\text{Diode \#2: } 1.34 \times 10^{-11} \text{ amps (167 on Range 4)}$$

$$\text{Diode \#3: } 1.17 \times 10^{-11} \text{ amps (144 on Range 4)}$$

$$\text{Diode \#4: } 3.10 \times 10^{-8} \text{ amps (154 on Range 2)}$$



4.3.5 Noise and Offset

In system tests at RCA we observed that noise in the diodes was gaussian, at the following levels:

Diode #2: $\pm 6.1 \times 10^{-14}$ amps (± 122 mv) 1σ
Diode #3: $\pm 3.5 \times 10^{-14}$ amps (± 70 mv) 1σ

This is the uncertainty expected in a single data sample, and we get four samples per second from each diode. Diode #2 is noisier than desired, but within the range of performance we can expect.

Using projected signal levels, the following noise to signal ratios are predicted:

<u>Filter</u>	<u>Signal</u>	<u>Noise (1σ)%</u>	
		<u>Diode #2</u>	<u>Diode #3</u>
OPEN	14×10^{-12} amps	0.4%	0.3%
Aluminum	7.1×10^{-12} amps	1.0%	0.5%
Tin	2.1×10^{-12} amps	3.0%	1.7%
Indium	1.6×10^{-12} amps	4.0%	2.0%

Offsets were measured during spacecraft-level testing in air at RCA. The following were observed:

	<u>Diode #2</u>	<u>Diode #3</u>
Hot (+35°C):	1.91×10^{-12} amp	5.9×10^{-13} amp
Cold (+5°C):	1.50×10^{-12} amp	1.4×10^{-13} amp



5.0 PHOTOMETRIC CALIBRATION

5.1 GENERAL

The photometric performance of the ESUM detection system can be characterized by the relation

$$S = E * A * T_g * \int_{\lambda} I(\lambda) * QE(\lambda) * F(\lambda) d\lambda$$

S = data signal

E = electronic conversions (Section 4.0)

A = detection area

T_g = Electrostatic grid transmittance

I(λ) = incident spectral irradiance from sun or test source

QE(λ) = detector quantum efficiency

F(λ) = filter transmittance

$\int_{\lambda} d\lambda$ = integration or summation over appropriate wavelength interval.

Photometric calibration of these parameters has been a joint GSFC/BBRC effort with separate areas of responsibility.

BBRC procured assembled and was responsible for calibration of the detectors; built and calibrated the electronics; measured and installed electrostatic grids; and assured general instrument photometric performance factors such as linearity, repeatability, etc.

GSFC procured and calibrated the filters, and performed the top level "integration" of the several calibration factors. GSFC also generated angular response functions based on orbital data.

The detection area factor was determined by the photocathode area of the ESUM-C EUV diodes and by filter apertures for the ESUM-C SEMS and ESUM-E EUV diodes.



BBRC provided technical support to the supportive calibration verification activity using calibrated diodes and filters to view the known flux from synchrotron radiation. That activity will not be covered here.

Because they are used only for engineering support, the Visible Light Diodes received markedly coarser photometric calibration than the primary science detectors.

5.2 ESUM-C CALIBRATION DATA

5.2.1 ESUM-C SEMS

The quantum efficiencies for the ESUM-C SEMS were determined at BBRC by comparison with NBS-calibrated EUV diodes and by comparison with flowing gas ionization chambers and geiger counters. The final data for the four flight SEMS are shown in Figures 5.2.1 through 5.2.4.

5.2.2 ESUM-C EUV Diodes

Calibration curves for the ESUM-C EUV diodes are shown in Figures 5.2.5, 5.2.6, and 5.2.7.

5.3 ESUM-E

5.3.1 EUV Diodes for ESUM-E

For ESUM-E, both of the flight EUV diodes were calibrated by the National Bureau of Standards, Gaithersburg, Maryland. The NBS calibration report is given as Figure 5.3.1.

The collecting area for the diodes is defined by precision apertures located in each filter. The machine diameter of the apertures is 0.197 ± 0.001 inches. This makes the detection area $0.197(\text{sic}) \pm 0.002 \text{ cm}^2$ for the Al, Sn, and In filters. The "open" filters

5/N 3041011 @ 2.00 1000

AR 0837-07

3 CYCLES X 10 DIVISIONS

SEMI LOG-ARITHM

Buffer time 100

5-2-73

QE

10.0

1.0

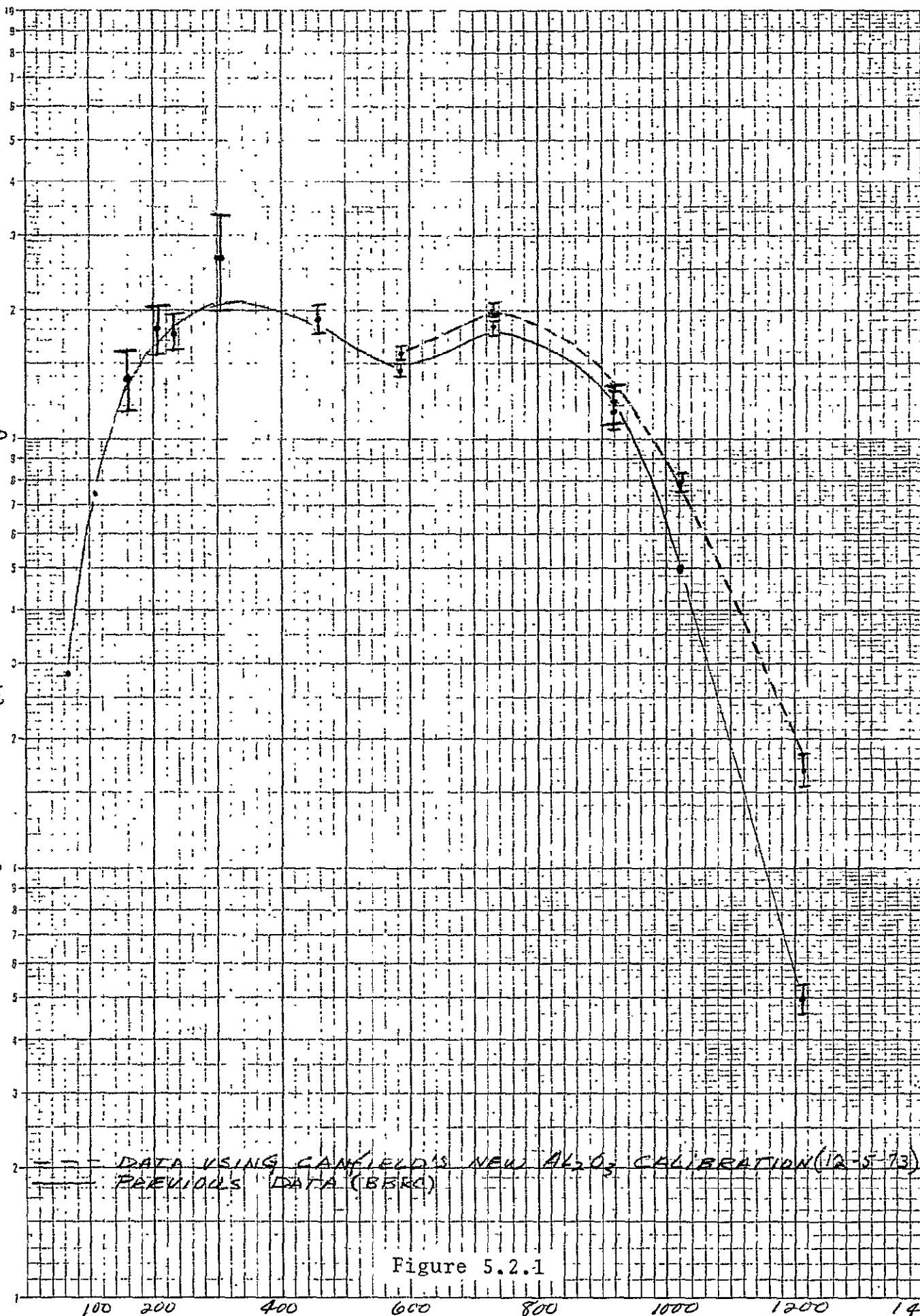


Figure 5.2.1

10.0

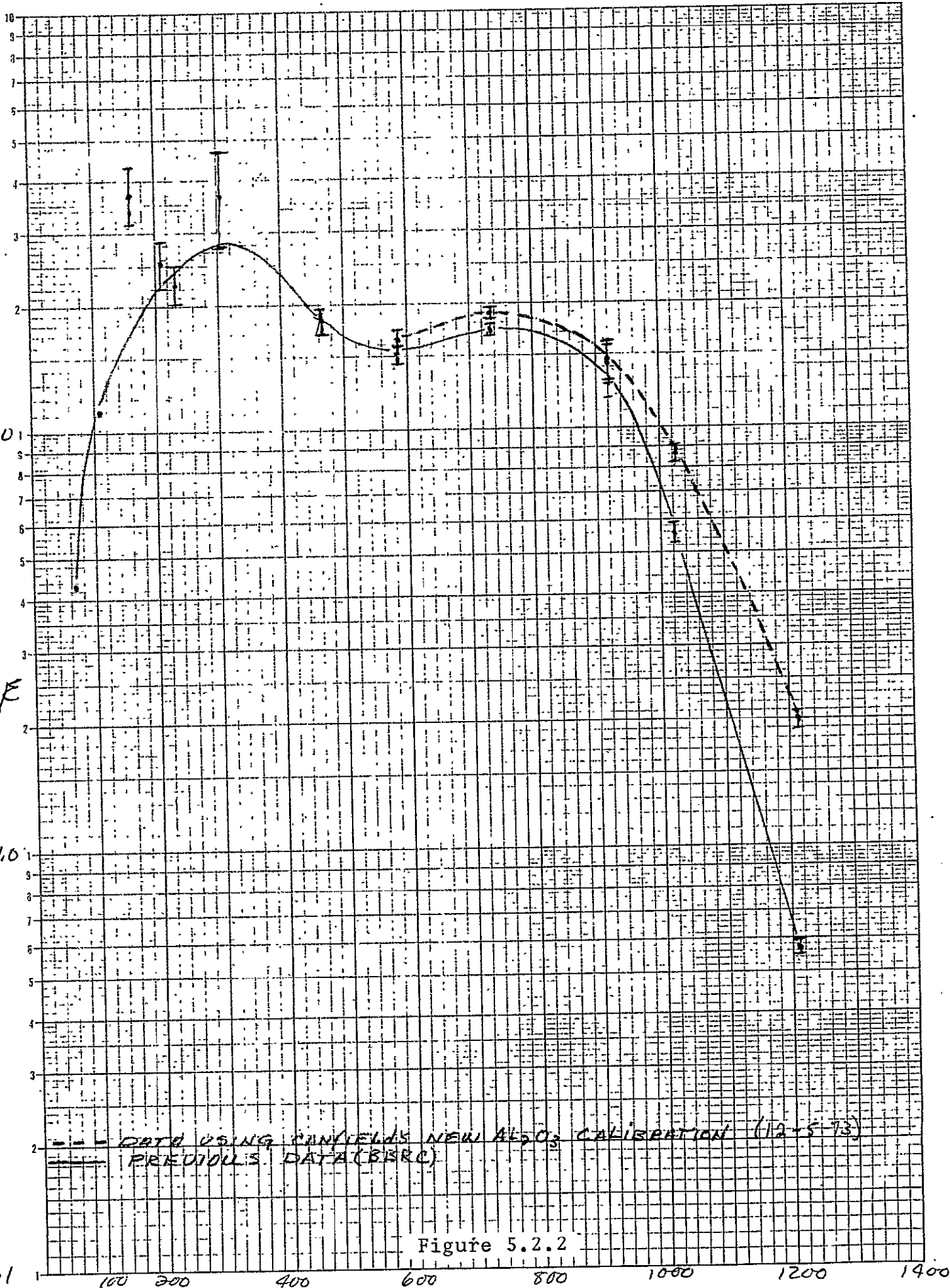
QE

1.0

--- DATA USING CONVEYOR'S NEW AL₂O₃ CALIBRATION (12-5-73)
 --- PREVIOUS DATA (BERC)

Figure 5.2.2

$\lambda(\text{\AA})$

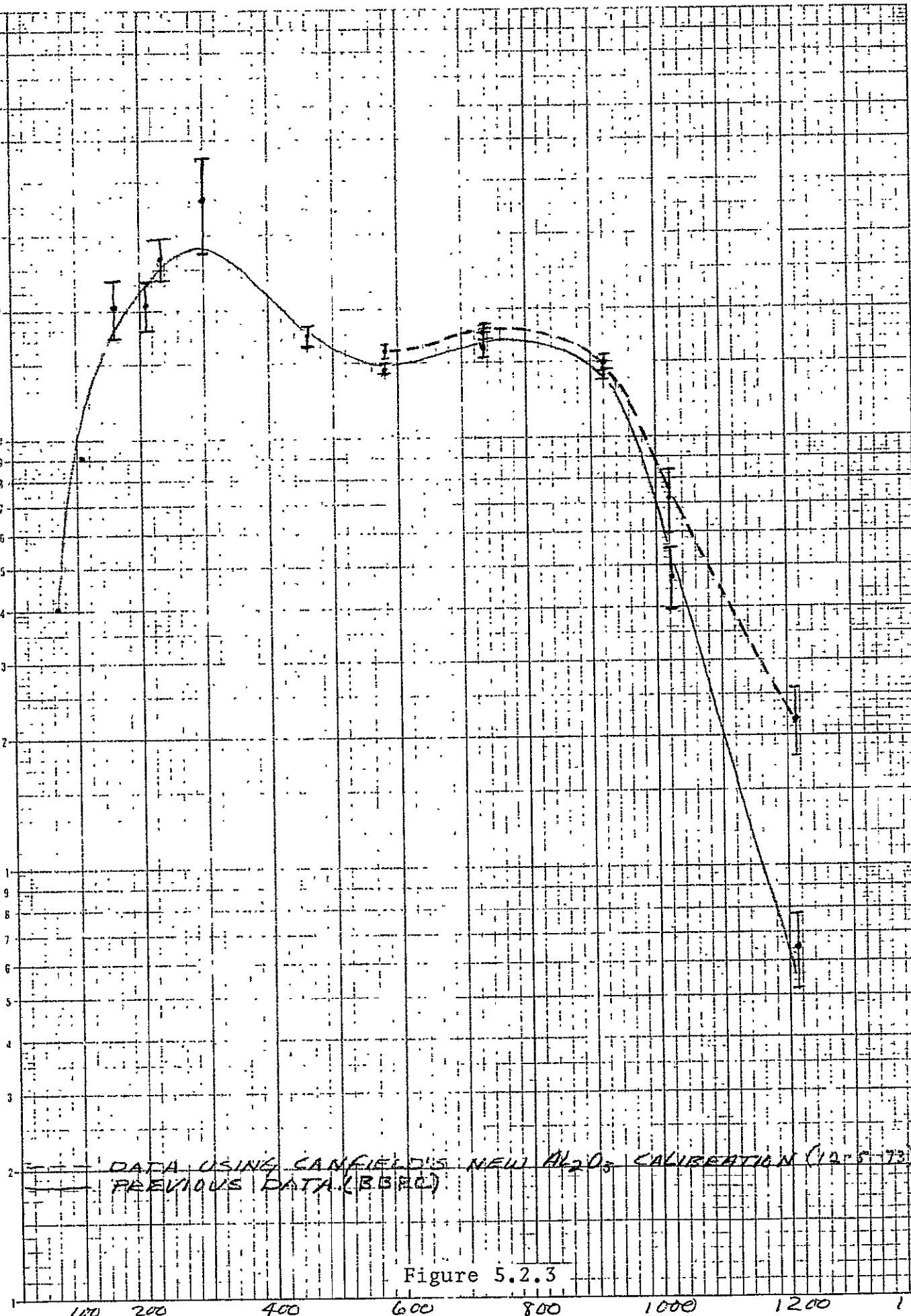


300 300 1140 10 510 11

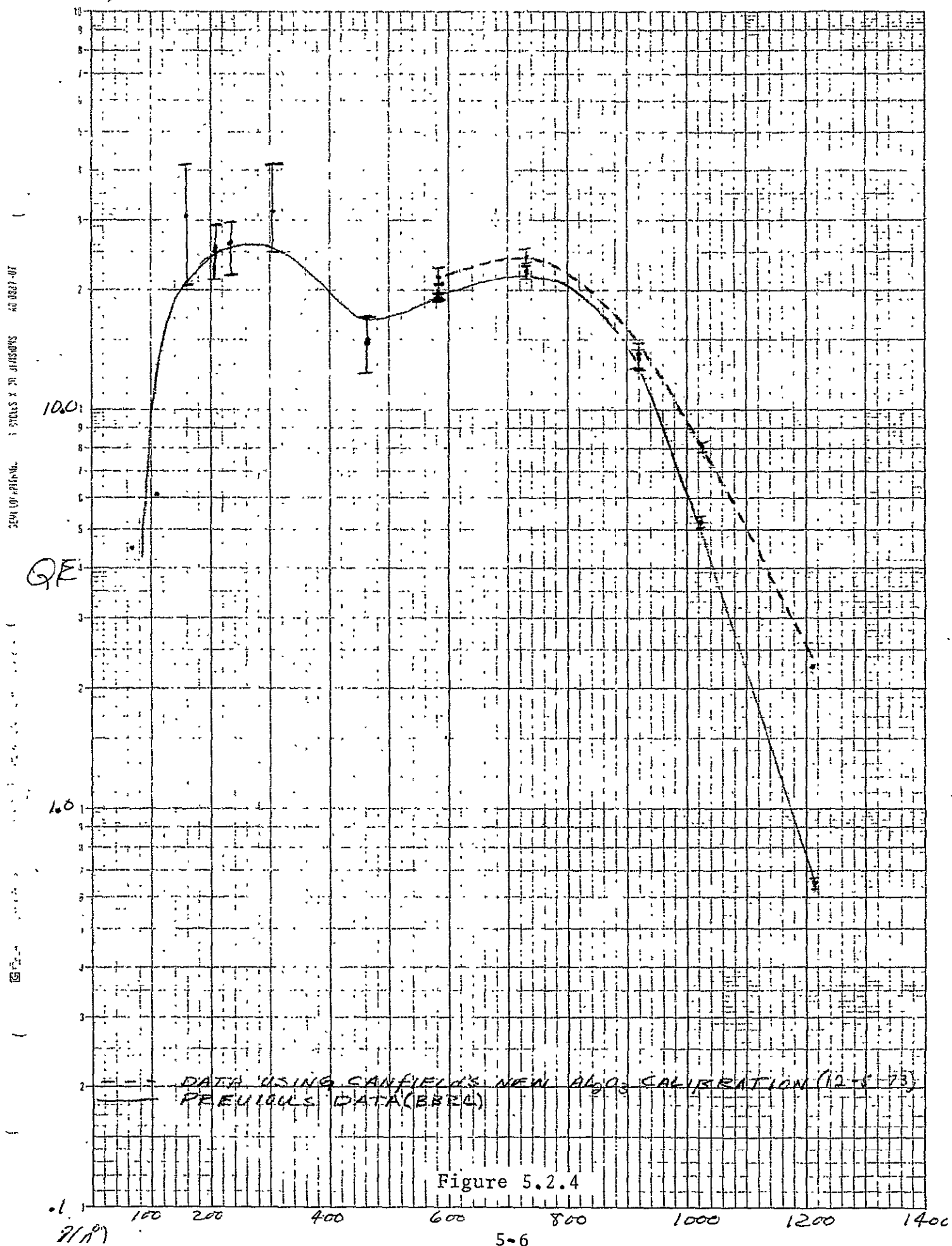
SEMI LOGARITHMIC 3 CYCLES X 10 DIVISIONS 10-0837-01

QE

1.0



SEM 5/N 3067101 (U) 21.01.73



HEATH LIGHT (REPLACEMENT)

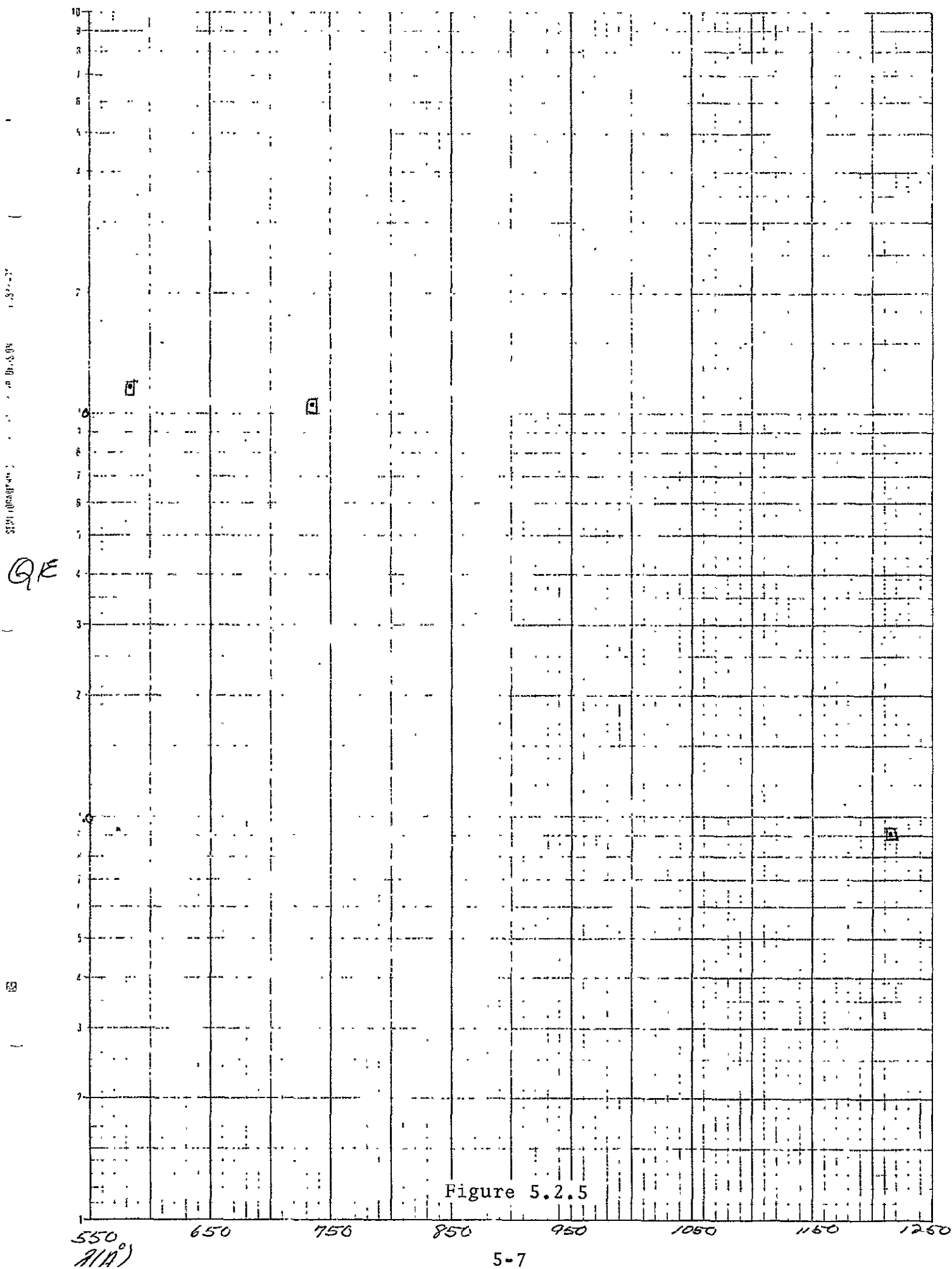


Figure 5.2.5

Q/E

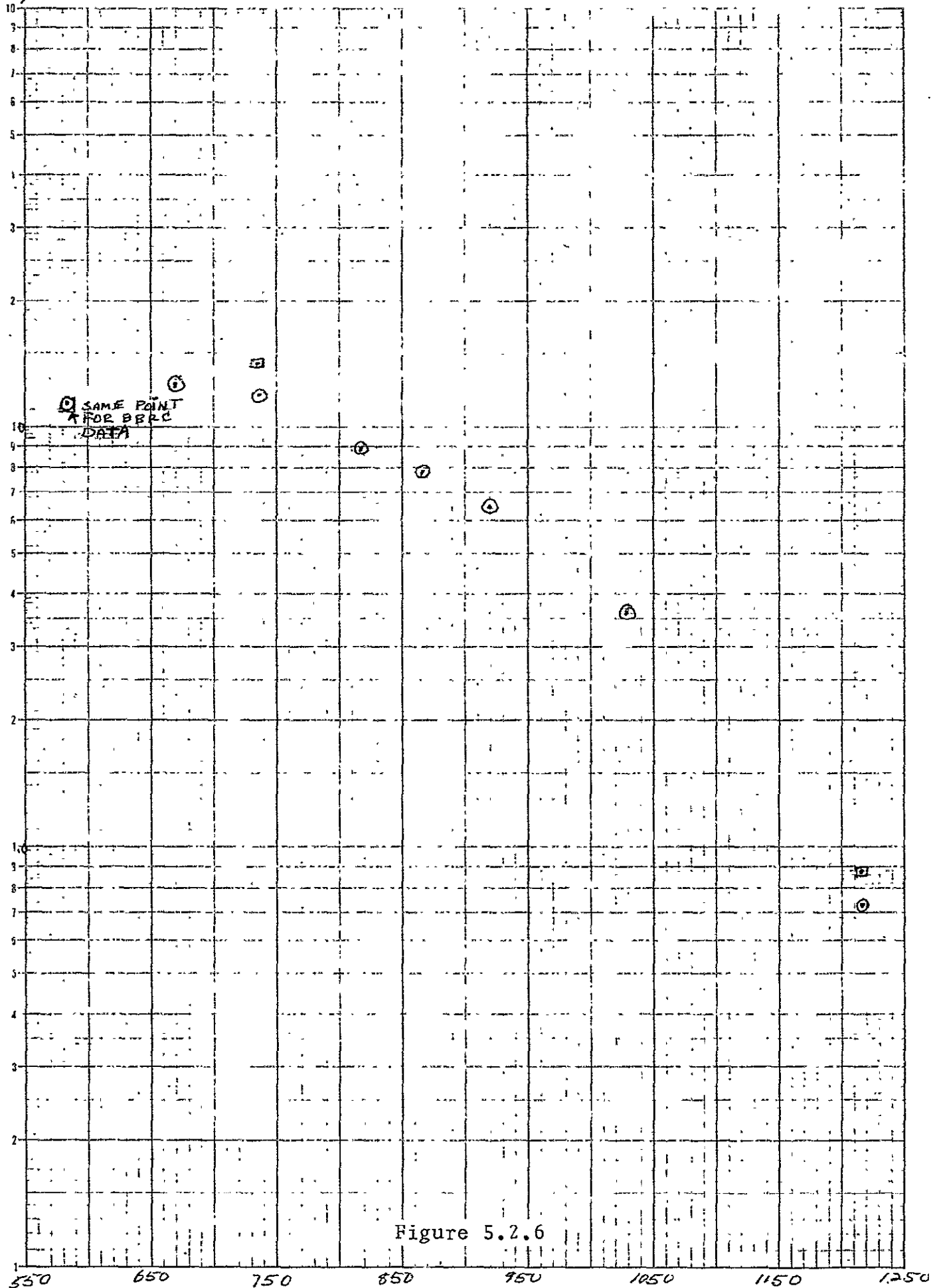


Figure 5.2.6

HEATH Diode 31N 123 Mos. #5.

BBRC DATA

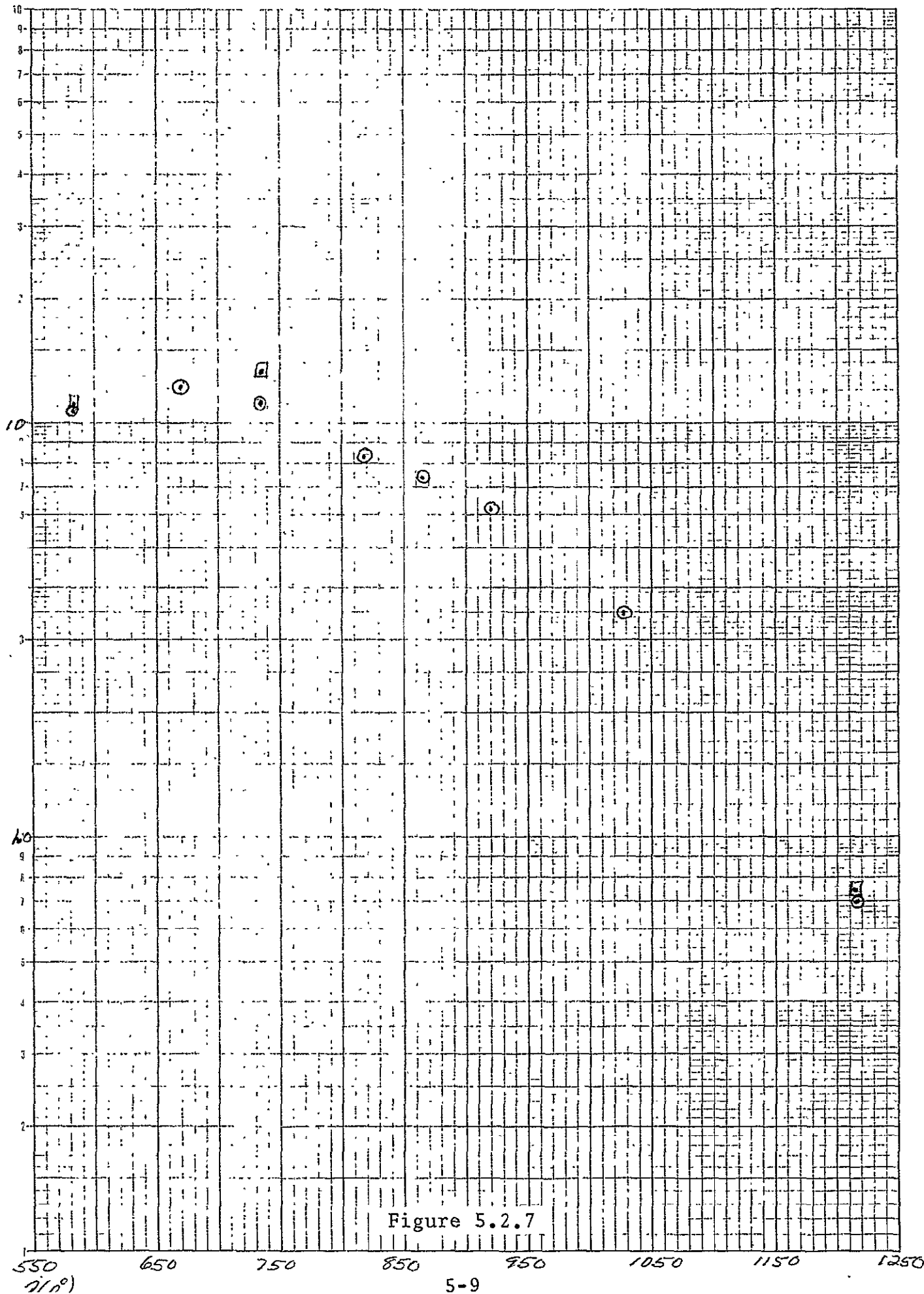


Figure 5.2.7

U.S. DEPARTMENT OF COMMERCE
NATIONAL BUREAU OF STANDARDS
WASHINGTON, D.C. 20234

232.03

REPORT OF CALIBRATION

April 26, 1974

for

Ball Brothers Research Corporation
Aerospace Division
P. O. Box 1062
Boulder Industrial Park
Boulder, Co. 80302

Ref: P.O. #40461
Attn: W. Nelson

Samples: Far ultraviolet detectors, NBS windowless photodiode serial no. 48, EMR windowless tetrodes, serial nos. 120 and 121. Most recent NBS calibrations: no. 48: 12/73 (informal), no. 120: 12/73, no. 121: 6/73.

Method of Calibration: Direct comparison of sample cathode photocurrents with those from an NBS-calibrated secondary standard windowless photodiode (200-1216Å) and windowed photodiode (1216-1487Å), with both sample and standard housed within the same vacuum chamber. The samples were not cleaned before calibrations.

The NBS sample (48) was operated with the anode +60V relative to the cathode which was at ground; photocurrent was measured in the cathode circuit.

The EMR samples (120,121) were operated with the supressor grid -30V and the anode +40V relative to the guard ring and cathode, which were at ground. Photocurrent was measured in the cathode circuit.

Calibrations were made using a plasma source for wavelengths 584-1487Å and an electron synchrotron for all wavelengths short of 584Å. The portion of the photocathode illuminated during measurements was 6 x 6mm to 10 x 2mm (no. 48 only).

The calibrations from 584-1216Å were performed before the shorter wavelength synchrotron calibrations and repeated afterward. Calibrations referenced to the windowed standard from 1216-1487Å were performed only after the synchrotron calibrations.

These calibrations were performed under the supervision of L. R. Canfield and E. B. Saloman, 232.03.

Figure 5.3.1

Results: (NBS photodiode no. 48, EMR tetrodes nos. 120, 121; 4/74)

Wavelength (Å)	Quantum Efficiency (%)				Probable Error (%)		
	48	120	121				
188	2.3	3.4	2.4			10	
208	2.8	3.8	2.8			10	
229	3.2	4.3	3.1			10	
250	3.7	4.8	3.5			10	
271	4.1	5.3	3.9			10	
292	5.0	6.3	4.8			10	
313	5.8	7.4	5.6			10	
333	6.5	7.8	6.0			10	
354	6.9	7.9	6.3			10	
375	7.4	8.2	6.7			10	
396	7.8	8.4	6.9			10	
417	8.1	8.4	7.1			10	
438	8.7	8.6	7.4			10	
458	9.1	8.8	7.6			10	
477	9.8	8.9	7.8			10	
500	10.1	9.0	7.9			10	
521	10.3	9.3	8.2			10	
542	10.6	9.9	8.8			10	
563	10.9	10.1	9.3			10	
	<u>a</u>	<u>b</u>	<u>a</u>	<u>b</u>	<u>a</u>	<u>b</u>	
584	10.7	10.7	10.4	10.5	9.06	9.82	8
669	11.7	12.0	11.2	11.2	9.50	10.3	10
735	12.6	12.9	10.5	10.5	8.93	9.68	8
818	12.3	12.6	8.22	8.33	7.32	7.96	8
865	11.4	11.8	7.33	7.39	6.48	7.08	8
920	9.71	10.0	6.16	6.22	5.43	5.94	8
1026	6.36	6.51	3.67	3.73	3.26	3.58	8
1216	2.24	2.25	0.972	0.985	0.787	0.874	6
1254		1.76		0.770		0.663	6
1354		0.722		0.310		0.261	6
1403		0.462		0.193		0.163	6
1441		0.317		0.133		0.109	6
1487		0.191		0.085		0.069	6

a) measured "as received"

b) measured "as returned"

Figure 5.3.1
(Continued)

Discussion: Each of the three detector samples was calibrated from 584-1216Å before and after the shorter wavelength synchrotron calibrations because experience has shown that some photocathodes undergo a change in quantum efficiency in the 584-1216Å region as a result of the shorter wavelength measurements. The "a" data sets should be most nearly representative of the quantum efficiencies at the time of receipt by NBS of the samples. The "b" data sets represent the quantum efficiencies at the conclusion of NBS measurements. (The measurements referenced to the windowed NBS standard, 1216-1487Å, were made only after the synchrotron calibrations, since the request to calibrate at these wavelengths was not made until the synchrotron calibrations were in progress.)

The data indicate relatively small changes in the quantum efficiencies, "a" vs "b", with the exception of sample no. 121. This sample appears to have relatively poor stability, based on the degree of change observed in its quantum efficiency values since the most recent previous calibration. (See Report of Calibration dated June, 1973.)

The quantum efficiencies quoted for 1216Å are the unweighted average of measurements using both windowless and windowed secondary standard detectors. An absolute difference averaging about 13% of the value was obtained consistently, independent of the sample being measured.

It should be noted that calibrations of windowless detectors at wavelengths longer than 1216Å is not a normal NBS procedure. No information concerning the stability of the quantum efficiency of $\text{Al}_2\text{O}_3/\text{Al}$ photocathodes is available. It would be expected that the stability would not be satisfactory due to the relatively low quantum efficiency in this region and the consequent domination of surface contaminants.

For the Director,

Robert P. Madden
Chief, Far UV Physics Section
Optical Physics Division

Figure 5.3.1
(Continued)

U.S. DEPARTMENT OF COMMERCE
NATIONAL BUREAU OF STANDARDS
WASHINGTON, D.C. 20234

232.03

REPORT OF CALIBRATION

December 16, 1975

for

Ball Brothers Research Corporation
Aerospace Division
Boulder Industrial Park
Boulder, CO. 80302

Ref: P.O. 21024

Attn: J. Buckley

Samples: Far ultraviolet detectors, EMR windowless photodiodes,
model no. 549-136, serial nos. 20,23 and 120.

Method of Calibration: Direct comparison of sample cathode photo-
currents with NBS-calibrated secondary standard windowless photodiodes,
with samples and standards housed within the same vacuum chamber.
The samples were not cleaned before calibrations. The sample anodes
were operated +40V and the suppressors -40V, both relative to the
cathodes, which were at ground potential. Photocurrent was measured
in the cathode circuit. The beam size on the cathode was 6 x 6 mm
(584-1216 Å) or 5 mm diameter (188-563 Å), centrally positioned at
normal incidence.

These calibrations were conducted under the supervision of L. R.
Canfield and E. B. Saloman, Section 232.03:

Figure 5.3.1
(Continued)

Results: (EMR photodiode, serial nos. 20,23 and 120, calibrated 9/75)

<u>Wavelength (Å)</u>	<u>Quantum Efficiency</u>			<u>Probable Error (%)</u>
	<u>20</u>	<u>23</u>	<u>120</u>	
188	.025	.030	.028	10
208	.027	.032	.032	10
229	.030	.037	.036	10
250	.033	.041	.040	10
271	.035	.044	.043	10
292	.038	.047	.047	10
313	.042	.051	.051	10
333	.045	.054	.055	10
354	.048	.058	.057	10
375	.051	.061	.061	10
396	.055	.063	.064	10
417	.059	.064	.064	10
438	.064	.063	.065	10
458	.068	.062	.062	10
479	.074	.062	.065	10
500	.080	.063	.070	10
521	.083	.067	.076	10
542	.086	.073	.083	10
563	.088	.083	.093	10
584	.0887	.105	.0999	8
669	.0915	.117	.106	10
735	.0912	.117	.103	8
818	.0745	.0866	.0808	8
865	.0633	.0720	.0690	8
920	.0547	.0612	.0608	8
1026	.0351	.0377	.0384	8
1216	.00844	.00782	.00967	6
1354	.00228	.00171	.00271	6

Discussion:

Sample no. 120 was, at the request of BBRC, also calibrated 584-1216 Å using the suppressor and anode voltages employed in a previous (6/74) NBS calibration of this sample. These voltages were +40V (anode) and -30V (suppressor).

Figure 5.3.1
(Continued)

The changes in the measured quantum efficiencies QE_1 (4/74) and QE_2 (9/75) using these voltages were:

<u>Wavelength (Å)</u>	$\frac{QE_2 - QE_1}{QE_1} (\%)$
584	-7.2
669	-7.1
735	-4.0
818	-6.3
865	-10.0
920	-5.8
1026	-1.6
1216	-0.99

Samples 20 and 23 show visible evidence of contamination, probably resulting from previous in-vacuum electrical accidents which are suspected by BBRC and NASA personnel. The influence of any such contamination on the stability of the quantum efficiency of such a device cannot be predicted.

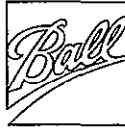
Sample 23 also exhibits abnormally low resistance from the photocathode to the guard.

For the Director,

Robert P. Madden

Robert P. Madden, Chief
Far Ultraviolet Physics Section
Optical Physics Division

Figure 5.3.1
(Continued)



were fabricated at BBRC with measured aperture diameters of 0.0810 ± 0.0001 inches, (area = 0.333 cm^2).

The outer mask covers each detector with a coarse screen grid. The screen has wires 0.0072 inches wide with square apertures 0.045 inches open width. Calculated transmittance is 0.73 .

5.3.2 Visible Light Diode for ESUM-E

The visible light diode has a response to the full sun of $5 \times 10^{-3} \text{ amps/cm}^2$. The filter areas (0.2 cm^2) would give 10^{-3} amps for a 100% leak. Thus 10^{-6} leak would be 10^{-9} amps.

The electronics were set to give one bit on the most sensitive scale to be $10^{-10} \text{ amps} = 10^{-7}$ pinholes.



6.0 INSTRUMENT PHOTOMETRIC TESTS

6.1 GENERAL

For system level photometric testing, ESUM is fitted with a test filter wheel and installed in BBRC COMBO Thermal Vacuum Chamber. A windowless gas discharge source is mounted on the chamber wall, separated from the instrument by approximately two meters. Tests are run with the lamp filled with H₂, He, Ne, Ar, Kr, and Xe, each run at a variety of lamp currents. Data from the various detectors and test filters are then analyzed for stability, consistency, linearity, and relative response.

The temperature control capability of the chamber is used to verify operation at extreme temperatures.

In general, test filters consist of flight-configuration mounts with varying aperture sizes and no metallic filter material. This design is intended to allow detector linearity and repeatability tests. Spectral response comparisons can be made because of the spectral purity of the dominant emission lines of the various gases.

The goals of the photometric testing program were to investigate instrument operation to accuracies of 1% or better. Unfortunately, the characteristics of the discharge lamp prevented reliable analysis of all tests to this level.

The distribution of the lamp's output is not uniform over the entire face of ESUM, and varies with lamp gas, gas pressure, and current. The exact distributions in the test geometry have not been mapped. However, data from ESUM show variations over the various detectors of factors of two from setup to setup, and 10-20% variations among various runs in a given setup.



A second lamp difficulty is that it does not accurately model the sun. The lamp appears as a point source, only 1.2 milliradians in diameter, compared to the sun at 10 milliradians. Further, the sun will sweep across ESUM's field of view as the spacecraft rotates; the test setup is static. Thus, it is not possible to identify localized irregularities in grid material or angular variations in detector efficiency in test.

6.2 TESTING OF ESUM-C

6.2.1 Test Configuration

For test purposes, the filters for EUV diodes 2 and 3 were replaced with filter frames fitted with 90% transmitting mesh. This is equivalent to removing the thin film of Sn or In from the flight configuration filters. EUV diode #1 was equipped with the same 90% filter, as it was in Flight.

The SEM filters were replaced with test filters incorporating 5% mesh (as in flight configuration) and four different apertures: nominal aperture diameters were .036, .047, .073, .086 inches. An Fe^{55} source and three solid blanks completed the filter wheel and detector, and the relation of filter position to telemetered wheel position.

6.2.2 ESUM-C Testing of 27 September 1973

On 27 September 1973 ESUM-C underwent its first successful photometric testing. The instrument was tilted at 10° to the incident light, and centered in the beam from a filament lamp held in place of the gas lamp.

Table 6.2.1 summarizes the conditions of the discharge lamp (gas, pressure, voltage, and current) for each of the recorded runs. The filter wheel was stepped through one revolution on



Table 6.2.1
ESUM-C Photometric Tests
of
27 September 1973

<u>RUN</u>	<u>GAS</u>	<u>PRESSURE</u> (mm)	<u>VOLTAGE</u> (volts)	<u>CURRENT</u> (ma)
1	Neon	0.7	500	75
2	Neon	0.7	550	100
3	Neon	0.7	625	150
4	Neon	0.7	750	200
5	Neon	0.7	1150	250
6	Neon	0.7	1250	300
7	Neon	0.7	1550	400
8	H ₂	2.0	650	75
9	H ₂	2.0	800	150
10	H ₂	2.0	925	200
11	H ₂	2.0	1025	250
12	H ₂	2.0	1100	300
13	H ₂	3.0	1225	350
14	Ar	0.2	500	75
15	Ar	0.2	875	150
16	He	1.0	550	75
17	He	1.0	600	100
18	He	1.0	750	175
19	He	1.0	950	250
20	He	1.0	1200	350
21	He	0.3	1575	425
22	Kr	0.2	1250	250
23	Kr	0.2	1600	400
24	Kr	0.15	1050	150
25	Xe	0.15	925	200
26	Xe	0.15	650	100
27	Xe	0.15	1250	300
28-32	Fe ⁵⁵ - H.V. LEVEL TESTS			
33-36	He	1.0	750	100
(H.V. LEVEL TESTS)				



each run, dwelling approximately five seconds at each position.

SEM data were manually reduced from the printer paper. Twelve samples (.25 seconds each) were averaged. The averages were then checked back against the raw data to catch any glaring reduction errors. Diode data were similarly averaged, then converted to current levels.

The results of the photometric tests were summarized in Table 6.2.2. Runs 28-36, involving high voltage level tests, are summarized in Table 6.2.3. Note in particular the highly consistent and repeatable Fe^{55} data.

Several general comments can be made:

- The instrument worked.
- Variations among the three diodes were indicative of changes in the lamp distribution for the various pressures and lamp currents. This was most dramatic for the very low pressure Xe discharge runs.
- The general trend to lower SEM-to-diode ratio as lamp current increases was attributed to a broadening of the lamp distribution, i.e., more light is falling in the diode areas near the edge of the beam as the current increased.
- Aperture #2 produced erratic counts, especially for SEM's 1 and 2. We tentatively attributed this to a Moiré/diffraction effect. See data from 1 November 1973 for more detail.

Table 6.2.2

RUN	APERTURE #1 (0.036 in. dia.) SEM			APERTURE #2 (0.047 in. dia.) SEM			APERTURE #3 (0.72 in. dia.) SEM			APERTURE #4 (0.086 in. dia.) SEM			Fe ⁵⁵ SEM			DIODE 1 x 10 ⁻¹³ Amp	DIODE 2 x 10 ⁻¹³ Amp	DIODE 3 x 10 ⁻¹³ Amp
	1	2	3	1	2	3	1	2	3	1	2	3	1	2	3			
Gas Ne																		
1	224	209	213	416	480	401	1091	1033	1327	1290	1205	1581	3320	3207	2708	84.5	79.3	70.1
2	308	264	268	539	480	547	1435	1361	1784	1591	1686	2113	3299	3219	2699	113	108	95.6
3	450	413	428	846	1005	820	2249	2095	2727	2624	2479	3223	3288	3119	2685	179	172	151
4	607	507	570	1185	922	1111	3135	3179	3502	3275	3257	4173	3295	3232	2710	235	229	199
5	829	796	768	1332	1271	1457	3813	3628	4689	4631	4337	5507	3322	3215	2682	292	320	271
6	957	825	884	1609	1402	1691	4528	4252	5673	5174	5026	6591	3320	3236	2681	351	379	318
7	1083	1003	954	1751	1626	1827	5130	4819	6077	5886	5642	7189	3315	3255	2696	392	422	359
Gas H ₂																		
8	444	387	390	807	541	758	2242	2020	2634	2528	2336	3023	----	3203	2696	154	153	134
9	733	645	771	1795	1869	1315	3650	3373	4413	4298	3002	4460	3303	3241	2695	235	273	236
10	926	906	958	1323	1256	1697	4585	4249	5516	5577	4995	6006	3305	3202	2713	308	353	301
11	1123	1094	1067	1447	3301	1982	2417	5045	6318	6594	5937	6490	3292	3232	2724	373	425	366
12	1363	1238	1119	1641	1601	2317	6613	5852	7437	7486	6924	8351	3287	3209	2681	442	500	427
13	1584	1175	1287	3828	1729	2610	7241	6708	9714	8438	7841	8708	3314	3234	2713	518	575	492
Gas Ar																		
14	233	186	225	442	235	426	1051	953	1366	1278	1122	1408	3306	3192	2719	690	712	608
15	327	313	269	588	487	543	1154	1405	1883	1728	1719	1812	3307	3207	2702	107	106	95.6
Gas He																		
16	100	98	97	188	108	188	488	448	592	544	541	731	3320	3213	2731	34.5	32.5	28.7
17	135	127	141	221	244	253	700	623	823	785	751	1060	3337	3215	2705	47.1	46.9	41.0
18	266	258	275	396	372	471	1261	1268	1516	1380	1389	1739	3317	3267	2713	94.1	93.3	80.6
19	403	378	410	841	1121	739	2068	1795	2393	2375	2155	2857	3303	3207	2722	144	145	128
20	480	499	590	993	685	950	2595	2404	3075	3097	2882	3446	3315	3236	2710	166	198	174
21	711	740	735	1447	1207	1361	3960	3688	4245	4743	4317	4833	3314	3228	2712	286	338	302
Gas Kr																		
22	80	69	81	110	239	153	405	360	490	558	433	522	----	3231	2682	25.1	24.8	23.6
23	154	154	137	287	220	261	745	688	936	887	791	956	3317	3209	2737	47.1	47.3	44.3
24	70	55	62	102	87	101	306	280	349	378	339	389	3345	3212	2685	18.8	19.0	17.0
Gas Xe																		
25	11	14	14	17	29	25	71	72	69	80	79	82	3376	3285	2714	0	1.9	5.8
26	5	9	5	11	13	12	32	32	35	38	38	42	3343	3267	2751	0	.7	2.9
27	51	61	80	104	85	209	309	453	346	616	369	446	3360	3269	2746	9.4	10.1	23.2
*SEM Data are counts/.25 sec																		
6-5																		

ORIGINAL PAGE IS
OF POOR QUALITY

Table 6.2.3

[illegible]

~~ORIGINAL PAGE IS
OF POOR QUALITY~~



- The relative count ratios among the various SEM's and apertures have variations and inconsistencies of 10% to 20% or so. Since the apertures don't change size from run to run, since SEM quantum efficiencies should not change up and down erratically and since the Fe^{55} data show continued stable detector operation, we can guess that the inconsistencies are related to lamp pattern and Moiré/diffraction effects.

6.2.3 ESUM-C Test Results of 1 November 1973

On 1 November 1973, ESUM-C underwent its second and final series of photometric tests. The instrument and test configuration were the same as for 27 September 1973.

Instrument modifications between the two tests included:

- Increased SEM discriminator thresholds to eliminate cross-talk at elevated temperatures.
- Repair of filter wheel coupling, including disassembly and reassembly of filter wheel subsystem.

Table 6.2.4 summarizes the lamp conditions for each of the recorded runs. Data were reduced as before.

Testing began with the instrument at approximately 50°C. The temperature gradually approached 20°C during the runs.

Table 6.2.5 shows the data collected during runs 1-21 on 1 November 1973. Note that the counts are sums of 10 readouts of data, of 0.25 seconds each. (27 September 1973 data were averaged over 12 readouts.)



Table 6.2.4
ESUM-C PHOTOMETRIC TESTS
OF
1 November 1973

<u>RUN</u>	<u>GAS</u>	<u>PRESSURE</u> <u>(mm)</u>	<u>VOLTAGE</u> <u>(volts)</u>	<u>CURRENT</u> <u>(ma)</u>
1	Background	---	---	---
2	H ₂	2.0	600	75
3	H ₂	1.5	750	150
4	H ₂	2.0	850	200
5	H ₂	1.5	975	250
6	H ₂	1.3	1075	300
7	H ₂	1.0	1175	350
8a-HV1	H ₂	1.3	1075	300
8b-HV2	H ₂	1.3	1075	300
8c-HV3	H ₂	1.3	1075	300
8d-HV4	H ₂	1.3	1075	300
9a-HV1	H ₂	1.3	1075	300
Ca1 1				
9b-HV2	H ₂	1.3	1075	300
Ca1 1				
9c-HV3	H ₂	1.3	1075	300
Ca1 1				
9d-HV4	H ₂	1.3	1075	300
10	Ne	1.0	425	75
11	Ne	1.0	625	150
12	Ne	1.0	750	200
13	Ne	1.0	975	250
14	Ne	1.0	1075	300
15	Ne	1.0	1200	350
16	He	2.0	500	75
17	He	2.0	675	150
18	He	2.0	800	200
19	He	2.0	900	250
20	H ₂	1.4	800	150
21	H ₂	0.7	800	150
22a	H ₂	0.38	800	150
22b	H ₂			150
22c	H ₂			150
22d	H ₂			150
22e	H ₂			150
22f	H ₂			150
22g	H ₂			150
22h	H ₂			150
22i	H ₂			150
22j	H ₂	0.3	775	150

Table 6.2.5

RUN	APERTURE 1			APERTURE 2			APERTURE 3			APERTURE 4			Fe ⁵⁵			Diode #1 X 10 ⁻¹³ Amp	Diode #2 X 10 ⁻¹³ Amp	Diode #3 X 10 ⁻¹³ Amp
	1A	2A	3A	1B	2B	3B	1C	2C	3C	1D	2D	3D	1F	2F	3F			
Background																		
1													30717			0	0	0
H ₂																		
2	2604	2986	5540	2588	4600	9092	14279	17631	20873	17913	21910	23799	30537	31412	26272	80	167	164
3	4030	5063	9276	4595	6652	14610	25530	31020	35209	30222	27213	43194	30692	31832	26203	149	285	278
4	5998	6902	11212	18145	9272	19627	33611	39942	46252	40762	49755	50858	30714	31642	26081	157	375	364
5	7280	7927	14350	8889	14137	21184	39292	47974	55671	47133	57104	64383	30935	31469	25996	251	449	438
6	7574	8496	16259	8238	24168	24116	45258	53211	62423	53232	65838	72248	30914	31558	25862	248	500	492
7	8832	10097	17898	10656	21318	26913	49897	59179	67418	58786	72212	83803	30839	31541	26213	276	551	553
8a						24849				53027				31469		245	497	486
8b						25435				53478				31718		245	497	483
8c						25263				53969				31530		245	497	483
8d						25574				53866				31824		242	493	486
9a						24524				51554				31834		242	490	479
9b						24976				51772				31351		242	490	479
9c						25215				52990				31719		242	490	479
9d						25442				53367				32045		242	490	479
Ne																		
10	1429	1825	3415	2553	3104	5357	8535	10592	13386	10234	12512	15393	30695	31792	26467	53	117	112
11	3015	3121	5649	4477	6257	9161	16019	18853	24105	19001	23192	27567	31142	31608	26484	94	197	191
12	3599	3928	7653	5589	9681	11320	20474	24538	30241	24838	30455	33883	30955	31634	26139	119	252	243
13	5852	6337	13127	9820	12125	19081	33175	39329	48124	39678	49990	55338	31018	31697	26399	198	397	399
14	6593	7329	13718	12037	13366	22663	36254	43533	53609	44790	52856	60641	31249	31777	26097	236	461	447
15	7467	8429	15441	13601	16125	23835	43200	50628	58526	52054	61935	68010	30913	31545	26341	245	525	502
He																		
16	607	999	1507	1862	1297	2260	4020	5116	5469	4631	6150	6203	30872	31722	26096	22	48.2	47
17	1467	2218	3549	6667	2400	6037	9675	11363	12570	11911	13996	15536	31168	31760	26096	53	113	107
18	1986	2818	4696	5078	5405	7682	13373	15493	17445	15784	19322	21482	31134	31719	26299	75	155	142
19	2562	3891	6381	4188	4679	10433	17581	20458	22346	21693	25915	26880	31057	31426	26129	97	194	188
H ₂																		
20	4551	7032		7073	20841				39177			45003	31294			170	317	308
21a	4241	6529		4852	19822				34675			41047				154	287	281
21b	4357	6437		4723	7118				34687			41715				154	287	279
21c	4192	5957		4822	7631				34361			43701				154	285	279
21d	4056	5118		5529	6335				35542			40969				154	284	278
21e	3848	5080		4692	18937				35944			43353				154	284	278
SEM data are total counts/2.5 sec																		

Run 22 was executed specifically to examine the wide variation in aperture 2 data on SEMS 1 and 2. In addition, it contributes information in the general stability and repeatability of instrument operations. Table 6.2.6 shows the results of the ten filter wheel revolutions sampled in run 22. Each revolution is identified (22-A through 22-J). Data are again sums over 10 samples of 0.25 seconds each. The data are organized to show the four apertures and Fe^{55} counts for each detector.

Several observations were made:

- The instrument continued to work. There was no cross-talk or diode noise at elevated temperatures.
- Aperture #2 continued to be erratic.
- Diode 1 and SEMs 1 and 2 appeared to be poorly illuminated compared to Diodes 2 and 3 and SEM 3.
- Runs 8 and 9 demonstrated that SEMS 1, 2, and 3 were healthy: their pulse distributions were well above normal and CAL thresholds for the lowest HV levels.
- Run 22 shows that operation was stable and repeatable for the two largest apertures. Analysis shows the Moiré/diffraction effects should be largely blurred out for these apertures.
- While the Fe^{55} data from run 22 appeared to be more stable than Poisson statistics would predict, data from all runs together fit Poisson statistics very well.
- Comparing SEM 3 and EUV diode 3, which are close together and in a more uniform illumination, we got very good agreement with predicted sensitivities.

Table 6.2.6

RUN	APERTURE #1			APERTURE #2			APERTURE #3			APERTURE #4			Fe ⁵⁵		
	1	SEM 2	3	1	SEM 2	3	1	SEM 2	3	1	SEM 2	3	1	SEM 2	3
22a	3593	5652	8677	5851	14255	14283	23357	27821	31668	28311	33525	38715	30959	31517	26029
22b	3635	5553	8609	6026	5542	14077	22966	27909	31915	28000	33889	38309	30970	31478	26256
22c	3843	4741	8594	13600	9890	14077	22995	27970	31987	28124	33835	38000	31114	31438	26304
22d	3629	4844	8494	4990	5659	14203	23088	27263	31553	28171	33280	38194	31119	31554	26408
22e	3581	5119	8530	11091	6198	13811	22517	27414	31230	28234	33291	35445	30894	31452	26213
22f	3536	5504	8674	4858	20190	13753	22304	27371	30754	27871	32722	39936	31028	31136	26192
22g	3523	5460	8534	9156	5582	14176	22508	27489	30731	27866	33172	37574	31145	31340	26192
22h	3494	5549	8378	9657	24756	14144	22736	27825	31250	27311	32913	34856	30785	31288	25956
22i	3635	5558	8551	5960	5218	13889	22617	27589	31016	27863	32941	37785	31098	31461	26223
22j	3631	5668	8479	4487	9087	13842	22560	27361	31264	27166	33175	36584	31108	31347	26297
	36000	53648	85520	75676		140249	227648	27612	313368	278917	332743	375403	310225	314011	262070



6.3 ESUM-E PHOTOMETRIC TESTING

6.3.1 General

Testing of ESUM-E was simplified over ESUM-C in two important respects.

ESUM-E has only two EUV diode detectors, and no SEM's. This means long waits after pumpdown (3 days) were eliminated, and only 1/3 as much data were generated in test. Secondly, the experience gained in ESUM-C testing was used to plan and execute ESUM-E tests to best advantage.

The photometric test history of ESUM-E is shown in Table 6.3.1. The first photometric tests of ESUM-E were combined with thermal/vacuum acceptance in early 1975. The objective of these tests was to verify proper, repeatable performance at the high and low temperatures seen during the thermal vacuum cycle. Following integration and spacecraft-level testing, ESUM-E returned to BBRC in late summer 1975 to have calibrated EUV diodes installed for flight. A final set of photometric tests was performed on 2-3 October 1975 just prior to shipment for the 19 November 1975 launch of AE-E.

6.3.2 ESUM-E Photometric Tests January/February 1975

The principal photometric objective of these tests was linearity, since the EUV diodes were of non-flight calibration status. To express linearity, we subtracted dark current from observed signals, for each aperture and both diodes, then divided by aperture area to get a normalized measured "brightness" (i.e., amps/cm²). A baseline "brightness" was defined for each diode by averaging the "brightness" derived from the two largest apertures when they were in front of each diode.

Table 6.3.1
ESUM-E T-V/CAL TESTS 1975

RUN	DATE	TEMP °C	LAMP CNT. ma	LAMP PRESS. torr	CAL DIODE #2 x 10 ⁻¹⁰ amp	CAL DIODE #3 x 10 ⁻¹⁰ amp	NOTES
1	1/22/75	20	---	---	9	11.5	Saw variations with smallest apertures and explored before going to temperature.
2	1/22/75	20	---	---	4.3	6.0	
3	1/22/75	20	---	---	1.85(2.0)	2.81(2.75)	
4	1/22/75	20	---	---	12.5 (11.5)	16.5 (17.0)	
5	1/22/75	20	250	450	---	---	
6	1/22/75	20	95	450	6.19	8.2	
7	1/24/75	20	250	700	9.75	14.5	Replaced very small apertures.
8	1/24/75	20	103	700	6.5	7.8	
9	1/24/75	20	75	700	3.5	4.7	
10	1/27/75	41	250	500	15.0	16.8	Background
11	1/27/75	41	80	500	6.4	8.4	
12	1/27/75	-5	---	---	---	---	
13	1/27/75	-5	250	500	13(13)	17(17)	Background
14	1/27/75	-5	75	500	5.7(6)	8.2(8.9)	
15	1/27/75	-5	---	---	---	---	
16	1/31/75	-5	250	500	12.5(12)	16.5(17.2)	Background
17	1/31/75	-5	90	400	6(6)	8.5(8.7)	
18	1/31/75	-5	---	---	---	---	
19-1	2/1/75	39.4	250	500	11	16	
19-2	2/1/75	39.4	250	500	11.8	16.1	
20-1	2/1/75	39.4	80	500	5.9	8.5	
20-2	2/1/75	39.4	80	500	5.5	8.5	
23-1	2/3/75	Amb.	250	550	11.2	16	
23-2	2/3/75	Amb.	250	550	11	15.9	
24-1	2/3/75	Amb.	78	550	6.2	8.8	
24-2	2/3/75	Amb.	78	550	6.3	8.8	

Table 6.3.1
ESUM-E T-V/CAL TESTS 1975
(Continued)

RUN.	DATE	TEMP °C	LAMP CNT. ma	LAMP PRESS. torr	CAL DIODE#2 x 10 ⁻¹⁰ amp	CAL DIODE #3 x 10 ⁻¹⁰ amp	NOTES
1	10/2/75	Amb.	250	1.2 mm (He)	---	---	Turn-on record
2	10/2/75	Amb.	250	1.5 mm (Ne)	---	---	
3	10/2/75	Amb.	250	1.5 mm (Ne)	---	---	
4	10/2/75	Amb.	100	1.5 mm (Ne)	---	---	
5	10/2/75	Amb.	250	1.5 mm (Ne)	---	---	Check ½ steps Repeatability checks Repeatability checks Repeatability checks Repeatability checks Repeatability checks
6a	10/2/75	Amb.	250	1.5 mm (Ne)	---	---	
6b	10/2/75	Amb.	250	1.5 mm (Ne)	---	---	
6c	10/2/75	Amb.	250	1.5 mm (Ne)	---	---	
6d	10/2/75	Amb.	250	1.5 mm (Ne)	---	---	
6e	10/2/75	Amb.	250	1.5 mm (Ne)	---	---	
X	10/2/75	---	---	-----	---	---	Background level
7	10/3/75	Amb.	250	1.5 mm (H ₂)	---	---	



Then the percentage difference in brightness was calculated for each aperture in front of each diode. Table 6.3.2 gives the results. The largest apertures were always self-consistent. The medium apertures also were generally within 1% agreement. Only the small apertures saw significant variations, and these were felt to be the result of interference effects with the mask grid wires.

A second overall check was a comparison of EUVS-E normalized "brightness" levels with measured brightness levels taken with a reference EUV diode and external electrometer. Table 6.3.3 portrays the results of this comparison. Location of the reference diode is critical because of gradients in the illumination pattern from the lamp. We believe this is a major factor in the data spread. However, averaging all of the data points from Table 6.3.3, we find standard deviations in the brightness ratios of 7% for diode 2 and 2% for diode 3 over all hot, cold, and ambient cycles. Considering the many sources of variation in this test, we felt good about ESUM-E's tested performance.

Table 6.3.2
ESUM CALIBRATION SUMMARY

% Deviation From Average of Largest Apertures

Diode #2

Run		7-1	7-2	8-1	8-2	9-1	9-2	10-1	10-2	11-1	11-2
Small	1	1.6	3.9	2.2	3.2	-1.1	6.1	-3.5	.8	.9	.9
	5	1.6	1.9	-2.7	.7	-3.2	-5.5	.9	3.9	6.3	-.3
Med.	3	-.1	1.0	.8	1.1	0	.1	1.1	.7	3.6	3.8
	6	.4	.7	1.2	1.1	.1	.1	1.1	1.5	3.8	3.8
Large	4	.1	-.3	.2	0	-.2	0	0	-.4	0	0
	8	-.1	.3	-.2	0	.2	0	0	.4	0	0

Diode #3



Run		7-1	7-2	8-1	8-2	9-1	9-2	10-1	10-2	11-1	11-2
Small	5	-4.3	-4.5	-6.6	-6.3	-11.3	-10.6	-5.3	-5.5	-1.9	-4.1
	1	-4.6	-4.6	-7.1	-7.6	-8.5	-1.8	-3.5	-4.3	-3.1	-4.1
Med.	7	-.6	-.7	-.3	0	1.3	-1.3	-.7	-.8	1.3	-.1
	2	-2.1	-.7	-.3	0	1.3	-1.3	-.7	-.8	1.3	-.1
Large	8	.4	.6	.1	.1	.3	.4	.2	.6	0	.6
	4	-.4	-.6	-.1	-.1	-.3	-.4	-.2	-.6	0	-.6

Table 6.3.2
(Continued)

ESUM CALIBRATION SUMMARY

% Deviation From Average of Largest Apertures

Diode #2

Run		13-1	13-2	14-1	14-2	16-1	16-2	17-1	17-2	19-1	19-2
Small	1	.9	5.4	1.9	1.9	3.9	2.7	0	0	2.2	2.8
	5	4.0	4.9	-2.8	3.7	4.5	3.0	-1.8	1.0	2.2	.1
Med.	3	.9	1.1	-1.5	-1.5	.2	.2	.5	.7	1.2	.6
	6	.8	.5	-1.5	-1.5	.2	.2	.6	.6	.9	.6
Large	4	0	0	0	0	0	0	0	.1	.2	.1
	8	0	0	0	0	0	0	0	-.1	-.2	-.1

Diode #3

Run		13-1	13-2	14-1	14-2	16-1	16-2	17-1	17-2	19-1	19-2
Small	5	-4.5	-4.6	-9.7	-6.9	-6.0	-6.6	-8.4	-6.4	-4.5	-.2
	1	-6.0	-3.9	-6.9	-6.1	-7.0	-6.3	-11.2	-8.0	-4.5	-.2
Med.	7	-1.3	-.6	-.8	-.7	-1.1	-2.4	-1.0	-1.0	-1	-1.1
	2	-1.3	-.4	-.8	-.7	-.6	-1.2	.5	-1.0	-2.2	-.4
Large	8	-.1	-.2	-.2	0	.2	.3	0	0	.2	.2
	4	.1	.2	.2	0	-.2	-.3	0	0	-.2	-.2



Table 6.3.2
(Continued)

ESUM CALIBRATION SUMMARY

% Deviation From Average of Largest Apertures

Diode #2

Run		20-1	20-2	23-1	23-2	24-1	24-2				
Small	1	2.5	2.5	3.7	3.1	1.4	1.5				
	5	0.6	-2.7	3.3	4.9	0.7	-2.4				
Med.	3	2.1	2.1	0.1	0.08	0.5	0.1				
	6	2.3	2.3	0	0.08	0.3	1.0				
Large	4	0	0	0	0	0	-.1				
	8	0	0	0	0	0	.1				

Diode #3

Run		20-1	20-2	23-1	23-2	24-1	24-2				
Small	5	-4.5	-5.3	-5.2	-4.9	-7.6	-9.8				
	1	-2.6	0.5	-5	-5.7	-6.9	-7.1				
Med.	7	0.8	1	-0.6	-0.9	-0.4	-0.2				
	2	0.8	0.5	-2.8	-0.7	-0.02	-1.4				
Large	8	0	0	0.2	0.1	0.1	0.2				
	4	0	0	-0.2	-0.1	-0.1	-0.2				



Table 6.3.3

ESUM CALIBRATION SUMMARY

Diode #2

Run	Average (10^{-14} amp/cm 2)	Cal Diode (10^{-10} amp)	Ratio
7	8193	9.75	840
8	4516	6.5	695
9	2657	3.5	759
10	9875	15	658
10	(after)	(13.2)	(748)
11	4598	6.4	718
11	(after)	(5.8)	(793)
13	9991	13	769
14	4660	5.7	818
16	9466	12.5	757
17	4924	6	821
19-1	9258	11	842
19-2	9309	11.8	789
20-1	4605	5.9	781
20-2	4605	5.5	837
23-1	9455	11.2	844
23-2	9458	11	860
24-1	4844	6.2	781
24-2	4806	6.3	763

Diode #3

Run	Average (10^{-14} amp/cm 2)	Cal Diode (10^{-10} amp)	Ratio
7	11861	14.5	818
8	6698	7.8	858
9	3837	4.7	816
10	13922	16.8	829
10	(after)	(17.3)	(805)
11	6960	(8.4)	(829)
11	(after)	8.4	829
13	14158	17	833
14	7011	8.2	855
16	13545	16.5	821
17	7035	8.5	828
19-1	13210	16	826
19-2	13233	16.1	822
20-1	6946	8.5	817
20-2	6946	8.5	817
23-1	13396	16	837
23-2	13396	15.9	843
24-1	7238	8.8	823
24-2	7221	8.8	821

